THE WAVEGUIDE INVARIANT: SPATIAL INTERFERENCE PATTERNS IN UNDERWATER ACOUSTICS

Chris H. Harrison
Institute of Sound and Vibration Research
University of Southampton
Highfield, Southampton SO17 1BJ
United Kingdom
and
Centre for Maritime Research and Experimentation
Viale San Bartolomeo 400
19126 La Spezia
Italy

Introduction

"If you see some fringes, don't throw them away, they could be useful."

In long range underwater acoustics there is a simple quantity known as the waveguide invariant that tells you how acoustic spatial interference patterns change as you move a distant receiver horizontally away from a sound source. More than just a curiosity, this quantity is beginning to find naval applications. A particularly attractive point is that interference fringes or striations enable location or ranging of a distant sound source using just a single hydrophone. But before I say exactly how it works, there are three other apparently disparate phenomena which are closely related, and this relationship can be understood by thinking about them all in the time domain. Furthermore they help understand what the fringes depend on.

The first phenomenon I noticed when I was a teenager with "clip-clop-shoes" walking down a quiet paved street next to a feather-edged fence, the type with vertical overlapping planks. The surprise was that the steel-tipped heels no longer went clip, clop. Instead they went "pyank, pyonk… ". In other words the original click or delta function was turned into a rapid downward frequency sweep.

The second phenomenon is the well known similar effect when you clap your hands near the steps of the Mexican ziggurat of Chichen Itza (see Declercq, 2013). The echo is a also a downward frequency sweep.

While doing some noise experiments in the Mediterranean with underwater sound being monitored by loudspeakers in the ship's lab I witnessed the third phenomenon. This was a randomly occurring, isolated rather strange sound that was rather like a Walt Disney Goofy's gulp. You can reproduce this sound by trying to say "Eeyore" like a donkey but with your mouth shut! Incidentally it sounds much louder with your head under water! The similarity is that it is also a downward sweep but at a much lower starting frequency.

The cause of these sounds was allegedly distant oil-prospecting air guns heard through a multipath environment where rays zig-zag many times between sea surface and bottom before reaching the receiver. The impulse response of a single distant shot can be revealed by unravelling the zig-zags to make straight paths between a vertical array of source images and the actual receiver. For the time being assuming the sound speed to be constant, it is clear that the earliest arrivals are bunched up, but as time progresses the later arrivals get further and further apart. By analogy with the pitched buzz of a playing card on bicycle wheel spokes, this sequence of ever more separated clicks sounds like a rather buzzy downward frequency sweep. What's in common with all three phenomena is the effective row of sources of clicks, all more or less at right-angles to the main path. We can replace the column of image sources with the row of reflecting corners in the feather-edged fence or in the Chichen Itza steps.

More formally, the height difference between the receiver and source image is $2nH + \mu z_s + \nu z_r$ where n is an integer, H is the water depth, z_s and z_r are the true source and receiver depths, and μ and ν both take values of +1 and –1. So with sound speed c at range r in the small angle approximation the travel time delay after the first return $\tau_{n,\mu,\nu}$ is

$$\tau_{n,\mu,\nu} = (2nH + \mu z_s + \nu z_r)^2 / (2rc) \qquad (1)$$

The quadratic relationship between n and τ is responsible for the early bunching up of the impulses. If you don't have access to bicycle spokes or playing cards you can do just as well in Matlab by setting up an array of zeros at some sampling frequency and then overwriting with a one at each of the delays indicated above and listening to this irregularly spaced "row of spikes" with the function 'sound'. Subtle differences may be introduced into the nature of the sound by altering the detailed positions of the spikes through the source and receiver depths and also by altering their amplitudes according to reflection coefficients, angles, and so on. Figure 1 shows a typical impulse response generated this way.

The waveguide invariant β

This simple-minded ray explanation seems perfectly natural at audio frequencies in the air acoustics case, but it may come as more of a shock to physicists and mathematicians who work in underwater acoustics. Typically they are taught to find the relevant differential equation, choose the boundary conditions for the particular problem, and solve it some-

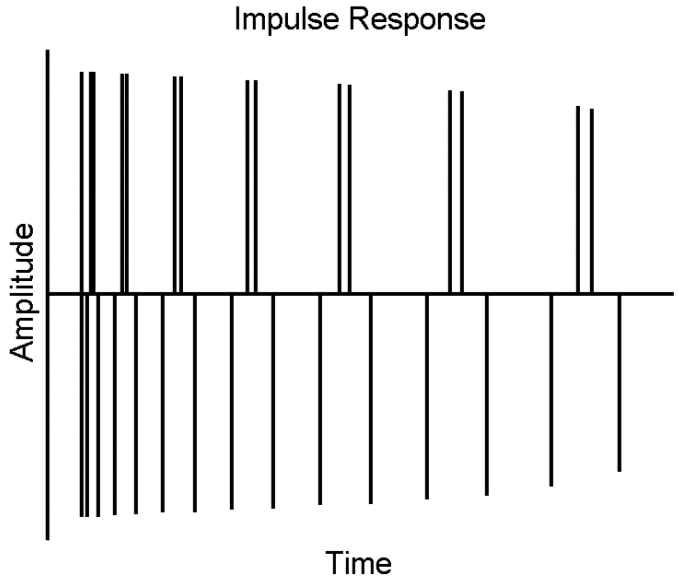

Fig. 1. A typical impulse response in a duct with initially bunched up arrivals (left) spreading out on the right. The groups of four, two-up-two-down, correspond to up/down paths at source and receiver with almost the same ray angle.

how. This will lead to the correct answer eventually but it may be much more heavy-going. Inevitably the solution is in the form of a Green's function in the frequency domain because that makes the differential equations easier to solve. Then in a ducted medium there are various choices of solution, for instance the Green's function can be expressed as a sum of vertical normal modes. However, if you want the impulse response, or to be precise, the waveform as a function of time, either you need to work out the group velocities for each mode then add the modes according to their arrivals, or you need to calculate the Green's function and modes for all frequencies and then Fourier transform them to time. As pointed out by David Weston (1971) there is a duality between rays and modes – if you include a large enough number of either rays or modes you will get the correct answer, but in any particular problem there may be a distinct computational advantage in choosing one or the other since a single ray is equivalent to many modes, and a single mode is equivalent to many rays. For instance, at low frequency and very long range there may be only a small number of modes but a very large number of rays [they may even be chaotic (Smith, et al, 1992)], so one would choose modes in that case.

The original work on the waveguide invariant (Chuprov, 1982) and most subsequent work (e.g. D'Spain and Kuperman, 1999; Brown, Beron-Vera, Rypina, and Udovydchenkov, 2005) took a frequency domain approach, using wave models of ducted sound propagation. The definition of the waveguide invariant, known as beta, in terms of angular frequency ω and range r is

$$\beta = \frac{d\omega/dr}{\omega/r} \tag{2}$$

which is also the slope of $d(\log\omega)/d(\log r)$. It is a property of, above all, the sound speed profile, and if this remains constant then β is a constant, i.e. invariant.

Lloyd's mirror fringes have been the basis of passive ranging for some time, and more generally striations are of interest because they can be measured with a single hydrophone. In recent years β has been considered as part of the toolset in geoacoustic inversion (Heaney, 2004) and has been applied to the detection of targets and reverberation estimation (Goldhahn, et al., 2008) and active sonar (Quijano, et al., 2008). It has also been tied into such topics as time reversal focusing (Kim, et al., 2003) and beam processing (Yang, 2003).

The waveguide invariant in a constant velocity duct

We can try to sweep away some of the mystique by using the impulse response crudely derived above but written more generally in Harrison (2011) and taking Fourier transforms. We can assume that at each n in Eq. (1), essentially each angle, the impulse has a slowly varying strength an determined by reflection coefficient, and so on, so the Fourier transform is

$$\begin{aligned} F(\omega, r) &= \int \sum_{\mu,\nu} \sum_{n} \delta(\tau - \tau_{n,\mu,\nu}) e^{i\omega\tau} d\tau \\ &= \sum_{\mu,\nu} \sum_{n} a_n e^{i\omega\tau_{n,\mu,\nu}} \end{aligned} \tag{3}$$

Although this is potentially a complicated function, by the time we have substituted for $\tau_{n,\mu,\nu}$ using Eq. (1) we see that the exponent is explicitly a function of (ω / r), so no matter what its dependence on n is or its functional form it has only one shape as ω and r vary. At any given r there will be a fringe pattern in ω, but moving to a different value of r we find the same pattern but stretched in ω in proportion to the increase in r. This automatically constructs a fringe pattern where the modulation takes a constant value along lines where $\omega \propto r$. In other words the condition for a fringe is that

$$\frac{\omega}{r} = A = \text{constant} \tag{4}$$

Taking logs and differentiating we find this obeys Eq. (2) with β = 1, as is well known for this isovelocity case. The result is an interference pattern that looks like that shown in Fig. 2.

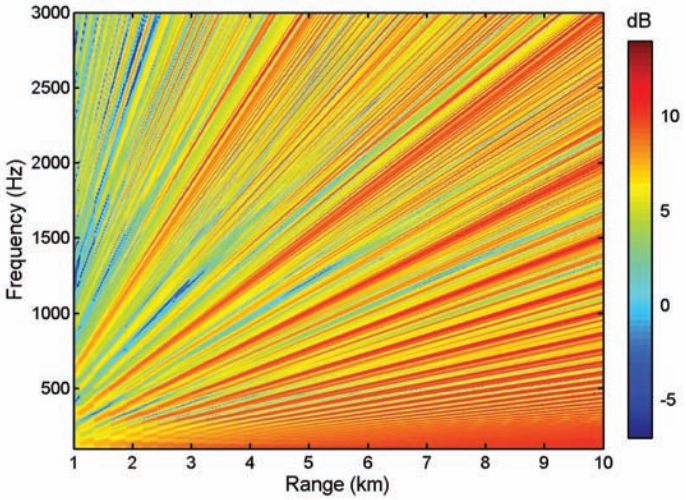

Fig. 2. An interference pattern ("striations") in water of 100m depth with constant sound speed. The waveguide invariant β = 1.

Why don't you see blobby interference patterns?

Why does the interference pattern in underwater acoustics always consist of parallel fringes (or striations) instead of just featureless blobs? The glib answer is, well, we've just proved it. But why? Think of other interference patterns such as directional gravity waves on the sea or normal modes on a drumskin or a bell – these often have features that, though not necessarily randomly blobby, are certainly not composed of parallel lines. In the *ideal* underwater case the source images are not just anywhere in the vertical plane, as they might be in room acoustics, but instead they form a relatively concentrated vertical array or grating subtending quite a small angle at the receiver. Therefore the streakiness of the fringes is just a manifestation of the diffraction pattern of a distant grating. On the other hand, suppose this were not an ideal case, for instance the sound speed might change spatially (or temporally) in an erratic manner, or there might be rough or wavy boundaries. Then the pattern is likely to break up, i.e. smooth out or tend to blobbiness. Perhaps this absence of a fringe pattern might also be a useful tool. The effects of internal waves on the stability of striation patterns has been studied by Rouseff (2001).

Some useful relationships

There are many other refracting sound speed profiles for which beta can be calculated analytically (see Harrison, 2011). To calculate them using this time domain approach we can make use of some rather surprising general relationships between modal quantities and ray quantities. In a sense these are all different interpretations of the same quantity T.

$$T = \frac{2}{\omega}\int \left[k(z)^2 - K^2\right]^{1/2} dz = \left(n - \frac{1}{2}\right)\frac{2\pi}{\omega}$$
$$= 2\int \frac{\sin\theta(z)}{c(z)} dz = t_c - \frac{r_c K}{\omega} = r_c\left(\frac{1}{U} - \frac{1}{V}\right) \quad (5)$$

Going through this term by term, the quantity T was referred to by Weston (1959) as a "characteristic" time. The normal modes propagate with horizontal wavenumber K and the modes themselves are solutions to the vertical Helmholtz equation with a vertical wavelength $[k(z)^2 - k^2]^{1/2}$, and the WKB solution is a good approximation to the mode shape.

The second term is known as the "WKB phase integral", the phase across the waveguide (multiplied by a factor $2/\omega$), and the third term is the condition that these modes fit into the waveguide, the integer n being the mode number – essentially a vertical resonance phenomenon. The characteristic time T is then the time equivalent of this phase.

Since locally the ray angle is given by $\cos\theta = k/K$ the second term can also be written as the fourth in terms of angle and sound speed. This quantity can be thought of as a *ray invariant* – it is useful for determining ray paths as they progress in range-dependent media, for instance if the water becomes shallower then the rays must become steeper in more or less the same proportion.

In a stratified or range-independent medium a ray starting at a particular angle cycles back and forth between upper and lower extrema, which may be refraction turning points or surface or bottom reflections, and it obeys Snell's law, which is equivalent to the horizontal wavenumber K being independent of depth. By considering the travel time along ray elements between extrema one arrives at the fifth term which relates T to the horizontal length of one complete ray cycle r_c and the corresponding travel time t_c. Noting that the group velocity U is just r_c / t_c since this is the speed that information travels along the waveguide, and the phase velocity V is by definition ω / K, we arrive at the last term (Harrison, 2012). This can be thought of as r_c times the difference between the group slowness and the phase slowness.

The waveguide invariant in a refracting duct

We can extend the argument that led to Eq. (4) to cover refracting environments. Equation (3) is still valid but the time delay τ_n is more complicated and it may even decrease with n (since the steeper rays tend to propagate mainly through the faster layers). To see fringes at all (i.e. sets of parallel lines rather than blobs) it must be possible to write τ_n as the product of a function of range only and a function of all the other parameters (e.g. n, H, z_s etc.). In other words in the exponent of Eq. (3) the range dependence must be separable. This ensures that in going from one range to the next the fringes may shrink or stretch slightly but always retain their shape. That property forms the striation pattern, and without it there can be no fringes.

The image arrival delay can be written in terms of $(t_c - r_c K/\omega)$ (which by coincidence is the "characteristic" time T) as

$$\tau_n = n\left(t_c - \frac{r_c K}{\omega}\right) \quad (6)$$

having dropped the source/receiver subscripts since we're interested only in the separation of the groups of four images. Although the right hand side is of the form $n\,G(r_c)$ this alone (in combination with $r = n \times r_c$) does not ensure that delay is a separable function of range r. The only function G that allows separation is $G(r_c) = g\,(r_c)^q$ (where g and q are constants), since $G(r_c) = G(r/n) = g\,r^q \times n^{-q}$. So to see fringes we *must* have

$$\left(t_c - \frac{r_c K}{\omega}\right) r_c^{-q} = g \quad (7)$$

and the exponent in Eq. (3) must be $i\omega r^q \times (n^{(1-q)} g)$. By taking logs of the latter and differentiating we find behaviour exactly as in Eq. (2) with $\beta = -q$. Doing the same to Eq. (7) we find a relation for β in terms of ray cycle distance and travel time

$$\beta = -\frac{\partial \ln\left(t_c - \frac{r_c K}{\omega}\right)}{\partial \ln(r_c)} = \frac{r_c^2 (dr_c/dK)^{-1}}{(\omega t_c - r_c K)} \quad (8)$$

It is now straightforward to plug in any sound speed profile, calculate r_c, t_c, K and calculate β, but straightaway we can see that the sign of β just depends on the dependence of cycle distance on angle. If cycle distance increases with angle β is negative, and vice versa.

Refracting examples

Using a standard propagation model (ORCA) run at many frequencies it is straightforward to see the interference

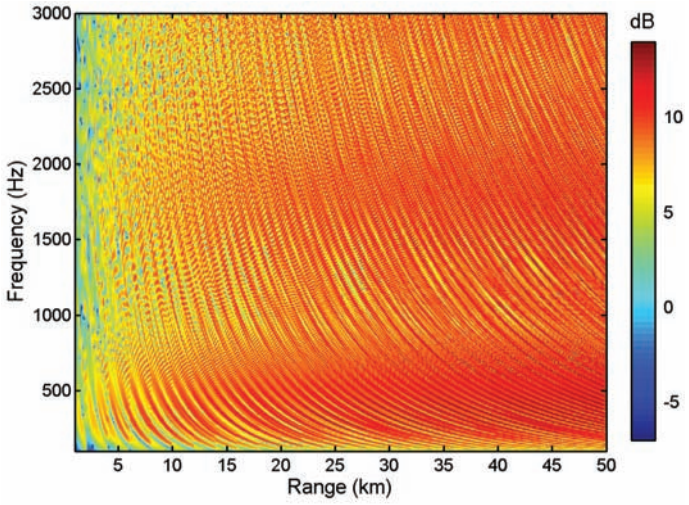

Fig. 3. An interference pattern with a uniform upward refracting profile in water of 100m depth. The waveguide invariant β = -3, and the striations bend in the opposite direction from those in Fig. 1.

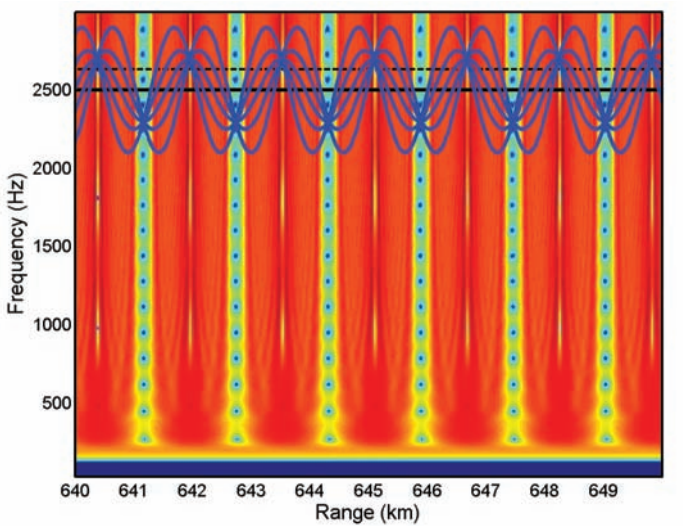

Fig. 4. Vertical fringes for the cosh profile where there is perfect focusing (as shown by the superimposed ray trace) which results in the ray cycle distance being independent of angle so that $\beta = \infty$. A raytrace is superimposed (blue).

fringes regardless of their shape. Figure 3 shows an example for the uniform sound speed gradient case where a and c_o are constants

$$c(z) = c_o(1 + az) \tag{9}$$

Using standard analytical techniques the cycle time and distance formulas are

$$t_c = \frac{2}{ac_o} \sinh^{-1}(\tan\theta_o) \tag{10}$$

and

$$r_c = \frac{2}{a} \tan\theta_o \tag{11}$$

where θ_o is measured at the low sound speed boundary. Here β = -3 and the fringes can be seen to tilt in the opposite direction to those in Fig. 1.

Another important case is the "cosh" profile

$$c = c_o \cosh az \tag{12}$$

which results in perfect, repeated focusing with

$$t_c = \frac{\pi}{ac_o} \tag{13}$$

and

$$r_c = \frac{\pi}{a} \tag{14}$$

By definition these perfect focuses mean that the cycle distance is independent of angle. In the context of interference fringes it sits on the dividing line between positive and negative values of β, and it is pathological since β is infinite, and the fringes, as shown in Fig. 4, are vertical, i.e. independent of frequency. Superimposed on this plot is a ray diagram showing the repeated upper and lower focus points. The horizontal dashed line shows the depth of the receiver used in the main plot.

Finally there is an interesting case of a parametrised profile that can display more or less all the properties of the others by altering a single parameter p.

$$c^2 = c_o^2 [1 + (az)^p] \tag{15}$$

(Actually, a very similar solution is also available for $c^2(z) = c_o^2/(1-(az)^p)$.) This can be imagined as a one-sided function with $0 < z < \infty$, in which case $z = 0$ represents a reflecting surface, or alternatively it can be imagined as a fully refracting, two-sided function with $-\infty < z < \infty$. Now the analytical solution for β is

$$\beta = \frac{p+2}{p-2} \tag{16}$$

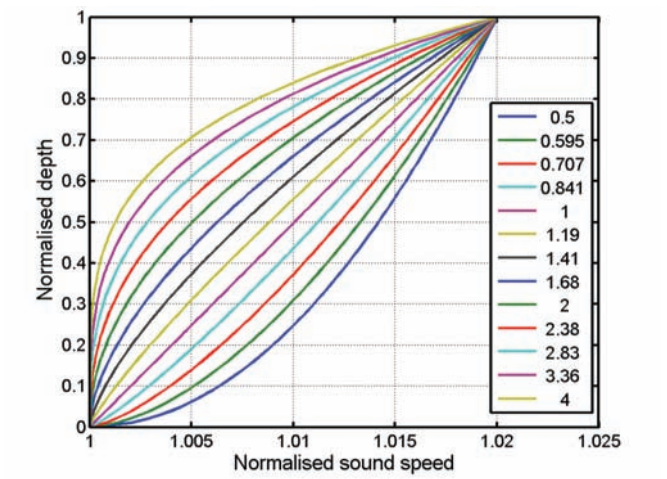

Fig. 5. Normalised sound speed profiles $c^2 = c_o^2(1+(az)^p)$ for various values of the parameter p for which solutions are available. These can be regarded as one-sided functions (with zero depth representing a reflecting surface), or alternatively as fully refracting two-sided functions.

If p is exactly 2 the function $k(z)$ is hyperbolic which is fairly close to the cosh case, and again $\beta \rightarrow \infty$. If p is greater than 2 then β is positive, and if it is less than 2, β is negative. If p is large then $k(z)$ remains flat but has a very sudden rise for $az > 1$, resembling a step in the sound speed profile or a reflecting surface. As one might hope, in the limit this results in $\beta \rightarrow 1$. If p is small then k rises rapidly for small z but then flattens out for large – this is not very likely oceanographically, but it results in $\beta \rightarrow -1$. An illustration of these profiles is shown in Fig. 5.

Conclusions

So the moral (to the signal processing fraternity) is, if you see some fringes, don't throw them away, they could be useful. In underwater acoustics the sound spectrum of a distant source may stretch or shrink as the receiver moves away. This leads to a streaky pattern of fringes or striations, and their gradient is quantified by the waveguide invariant β (Eq. 2). If the sound speed is constant then the fringes radiate from the source and $\beta = 1$. The limiting case of the cosh profile (Eq. 12) results in a repeated perfect focus for which $\beta \rightarrow \infty$. Generally the sign of β depends on whether the ray cycle distance increases or decreases with angle. If it decreases with angle then β is positive, as in the isovelocity case. If it increases with angle then β is negative as in the uniform gradient upward or downward refracting case where β is –3. Given some knowledge of the value of β and a moving platform there is promise of measuring ranges with a single hydrophone. AT

Acknowledgements

The author thanks Dr. Peter Nielsen for running the examples with the wave propagation model ORCA.

References

Brown, M. G., Beron-Vera, F. J., Rypina, I., and Udovydchenkov, I. A. (2005). "Rays, modes, wavefield structure, and wavefield stability," J. Acoust. Soc. Am., **117**, 1607–1610.

Chuprov, S. D. (1982). "Interference structure of a sound field in a layered ocean," in Ocean Acoustics, Current Status, edited by L. M. Brekhovskikh and I. B. Andreyeva (Nauka, Moscow, 1982), pp. 71–91, and (Joint Publications Research Service, Washington DC., 1985), pp. 88–111.

Cockrell, K. L., and Schmidt, H. (2010). "Robust passive range estimation using the waveguide invariant," J. Acoust. Soc. Am., **127**, 2780–2789.

Declercq, N.F. (2013). "On the fascinating phenomenon of diffraction by periodic structures", Acoustics Today, vol **9**, issue 1, p8-13.

D'Spain, G. L., and Kuperman, W. A. (1999). "Application of waveguide invariants to analysis of spectrograms from shallow water environments that vary in range and azimuth," J. Acoust. Soc. Am., **106**, 2454–2468.

Goldhahn, R., Hickman, G., and Krolik, J. (2008). "Waveguide invariant broadband target detection and reverberation estimation", J. Acoust. Soc. Am. **124**, 2841-2851.

Harrison, C.H. (2011). "The relation between the waveguide invariant, multipath impulse response, and ray cycles", J. Acoust. Soc. Am., **129**, 2863–2877.

Harrison, C.H. (2012). "A relation between multipath group velocity, mode number, and ray cycle distance", J. Acoust. Soc. Am., **132**, 48–55.

Heaney, K.D. (2004). "Rapid geoacoustic characterization: applied to range-dependent environments", IEEE J. Oceanic Eng. **29**, 43-50.

Kim, S., Kuperman, W.A., Hodgkiss, W.S., Song, H.C., Edelman, G.F., and Akal, T. (2003). "Robust time reversal focusing in the ocean", J. Acoust. Soc. Am. **114**, 145-157.

Quijano, J.E., Zurk, L.M., and Rouseff, D. (2008). "Demonstration of the invariance principle for active sonar", J. Acoust. Soc. Am. **123**, 1329-1337.

Rouseff, D. (2001). "Effects of shallow water internal waves on ocean acoustic striation patterns", Waves in Random and Complex Media, **11**:4, 377-393.

Smith, K.B., Brown, M.G., and Tappert, F.D. (1992). "Ray chaos in underwater acoustics", J. Acoust. Soc. Am., **91**, 1939-1949.

Weston, D.E. (1959). "Guided propagation in a slowly varying medium", Proc. Phys. Soc. London **73**, 365-384.

Weston, D.E. (1971). "Intensity-range relations in oceanographic acoustics", J. Sound & Vib. **18**(2), 271-287.

Yang, T.C. (2003). "Beam intensity striations and applications", J. Acoust. Soc. Am. **113**, 1342-1352.

Chris Harrison received his MA in Natural Sciences from Clare College, Cambridge in 1968. Subsequently, at the Scott Polar Research Institute, Cambridge he studied radio propagation in ice and spent two summer seasons in the Antarctic, completing his PhD in 1972. He started work in acoustics at Admiralty Research Laboratory, Teddington, and spent two years, from 1976 to 1978, as Exchange Scientist at Naval Research Lab, Washington where he worked on long distance reverberation in the Norwegian Sea. From 1978 to 1999 he worked as an acoustics consultant, mainly under contract to the UK MOD in a software company that is now a part of British Aerospace. His interests included development of propagation, noise, and sonar performance models. After joining the NATO Undersea Research Centre's (NURC) Acoustics Division in March 1999 he developed three experimental techniques from scratch to measure the seabed's reflection loss, sub-bottom layering, and geoacoustic properties using ambient noise and a drifting array. These were evaluated in a number of collaborative experiments south of Sicily. Simultaneously he developed the multistatic sonar performance model SUPREMO and the fast reverberation and sonar performance model ARTEMIS for use in tactical planning.

Chris was awarded the 1992 AB Wood Medal and the 2008 Rayleigh Medal by the UK Institute of Acoustics. He is currently a Visiting Professor at the Institute of Sound and Vibration, U. Southampton, and Emeritus scientist at the Centre for Marine Research and Experimentation (formerly NATO Undersea Research Centre), Italy. He is a Fellow of the ASA.